BMC Chemistry

RESEARCH ARTICLE

Open Access

# Crosslinked sulfonated polyacrylamide (Cross-PAA-$SO_3H$) tethered to nano-$Fe_3O_4$ as a superior catalyst for the synthesis of 1,3-thiazoles

Hossein Shahbazi-Alavi[1*], Sheida Khojasteh-Khosro[2], Javad Safaei-Ghomi[2] and Maryam Tavazo[2]

## Abstract

Crosslinked sulfonated polyacrylamide (Cross-PAA-$SO_3H$) attached to nano-$Fe_3O_4$ as a superior catalyst has been used for the synthesis of 3-alkyl-4-phenyl-1,3-thiazole-2(3*H*)-thione derivatives through a three-component reactions of phenacyl bromide or 4-methoxyphenacyl bromide, carbon disulfide and primary amine under reflux condition in ethanol. A proper, atom-economical, straightforward one-pot multicomponent synthetic route for the synthesis of 1,3-thiazoles in good yields has been devised using crosslinked sulfonated polyacrylamide (Cross-PAA-$SO_3H$) tethered to nano-$Fe_3O_4$. The catalyst has been characterized by Fourier-transform infrared spectroscopy (FT-IR), scanning electron microscope (SEM), dynamic light scattering (DLS), X-ray powder diffraction (XRD), energy-dispersive X-ray spectroscopy (EDS), thermogravimetric analysis (TGA) and vibrating-sample magnetometer (VSM).

**Keywords:** Polyacrylamide, Thiazole, Nanocatalyst, Nano-$Fe_3O_4$

## Introduction

1,3-thiazoles show anticancer [1], antimicrobial [2], anti-inflammatory [3], and anti-candida properties [4]. The synthesis of 1,3-thiazole derivatives have been developed in the presence of different catalysts including DBU [5], $HClO_4$-$SiO_2$ [6], $Bi(SCH_2COOH)_3$ [7], $[Et_3NH][HSO_4]$ [8], Ytterbium(III) Triflate [9] 2-pyridinecarboxaldehyde oxime [10] and potassium iodide [11]. The synthetic strategies of 1,3-thiazole derivatives were recently reviewed [12]. Despite the use of these ways, there remains a need for further new procedures for the preparation of 1,3-thiazoles. The modifying crosslinked polyacrylamides make them attractive objects in chemistry and polymer science [13–15]. Sulfonated polyacrylamides have unique characteristics such as high strength, hydrophilicity, and proton conductivity [16, 17]. Recently, magnetic nanoparticles (MNPs) have been successfully utilized to immobilize enzymes, polymers, transition metal catalysts and organocatalysts [18, 19]. Different stabilizers-electrostatic (surfactants), [20] or steric (polymers) [21–23] have been proposed to overcome the aggregation of magnetite ($Fe_3O_4$). In the current study, we investigated an easy and rapid method for the synthesis of thiazole-2(3*H*)-thione through three-component reactions of phenacyl bromide or 4-methoxyphenacyl bromide, carbon disulfide and primary amine using crosslinked sulfonated polyacrylamide (Cross-PAA-$SO_3H$) attached to nano-$Fe_3O_4$, as an efficient catalyst under reflux condition in ethanol (Scheme 1). A schematic representation of the catalyst is provided in Scheme 2.

## Results and discussion

### Characterization of the nanocatalyst

In this study, we synthesized the crosslinked sulfonated polyacrylamide (Cross-PAA-$SO_3H$) with simultaneous radical co-polymerization in presence of initiator and crosslinking agent. The FT-IR absorbance spectra of the dried crosslinked sulfonated polyacrylamide (poly AAM-*co*-AAMPS), $Fe_3O_4$ and Cross-PAA-$SO_3H$@nano-$Fe_3O_4$

*Correspondence: hossien_shahbazi@yahoo.com
[1] Young Researchers and Elite Club, Islamic Azad University, Kashan Branch, Kashan, Iran
Full list of author information is available at the end of the article

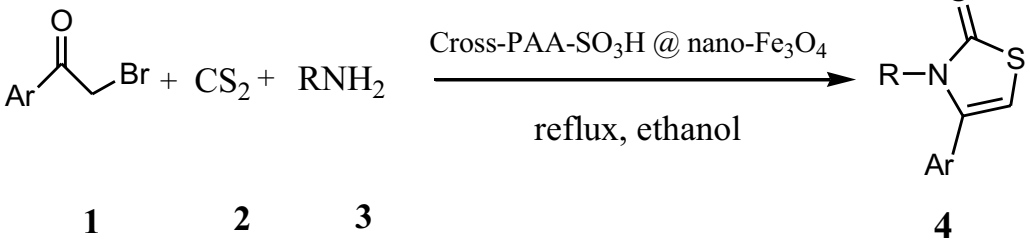


**Scheme 1** Synthesis of 1,3-thiazoles

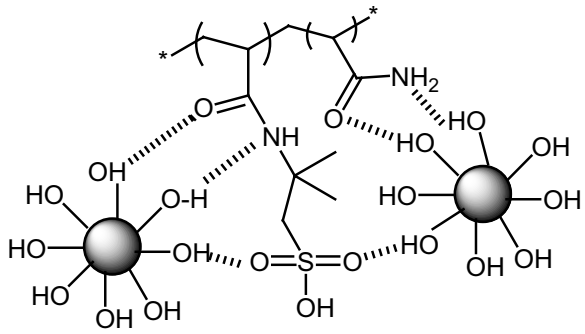


**Scheme 2** A schematic illustration for the formation of Nano $Fe_3O_4$@PAA-$SO_3H$

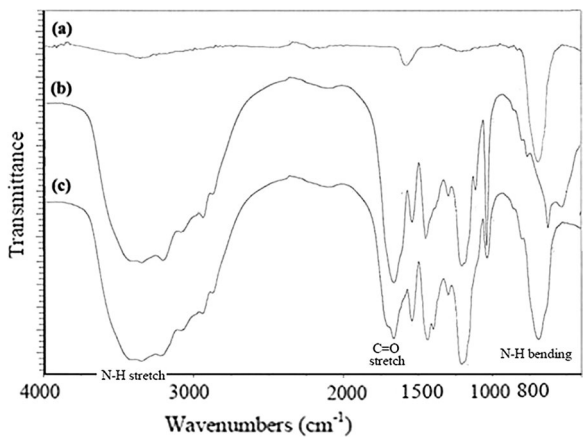


**Fig. 1** The FT-IR spectra of (a) $Fe_3O_4$ NPs, (b) Cross-PAA-$SO_3H$ and (c) Cross-PAA-$SO_3H$@ nano-$Fe_3O_4$

are shown in Fig. 1 (AAM is abbreviation acrylamide; AAMPS is abbreviation 2-acrylamido-2-methylpropanesulfonic acid).

The peaks at 3100–3500 $cm^{-1}$ are related to O–H (sulfonic acid group) and N–H (amide groups) in AAM and AAMPS. The strong band in the 1654 $cm^{-1}$ can be ascribed to the stretching vibrations of carbonyl groups in both AAM and AAMPS. The sharp peak at 1040 $cm^{-1}$ is related to sulfonic acid (–$SO_3H$) group. The bands at 700–800 $cm^{-1}$ and 1540 $cm^{-1}$ are related to the bending vibration of the N–H bond (primary and secondary amide respectively). Table 1 gives the main characteristic peak assignment of the FT-IR spectra. Meanwhile, a schematic illustration of the reaction is presented in the Scheme 3. The results in Fig. 1c suggest the integration of $Fe_3O_4$ NPs and Cross-PAA-$SO_3H$. The carbon nuclear magnetic resonance ($^{13}C$ NMR) of Cross-PAA-$SO_3H$ is displayed in Fig. 2. The peaks at 63.16 ($\underline{C}H_2SO_3H$), 46.83 ($\underline{C}HCONH_2$), 37.36 ($\underline{C}NHMe_2$), 34.23 (–$\underline{C}CH_2CO$), 29.15 ($\underline{C}H_2$), 22.91, 22.16 ppm (2 $\underline{C}H_3$), 18.14 ($\underline{C}H_2CHCONH_2$) are shown in Fig. 2. The $^{13}C$ NMR spectrum of the Cross-PAA-$SO_3H$ in DMSO-$d_6$ displayed two peaks at 176.36 and 173.89 ppm due to amide groups.

**Table 1 Peak assignment of crosslinked Sulfonated Polyacrylamide (Cross-PAA-$SO_3H$)**

| Peak position ($cm^{-1}$) | Assignment |
|---|---|
| 3100–3500 | N–H stretching of $NH_2$, OH stretching of (–$SO_3H$) |
| 1658 | C=O stretching of CO in AAM and AAMPS |
| 1545 | N–H bending (Secondary amid band of AAMPS) |
| 1042 | Sulfonic acid (–$SO_3H$) group |
| 1175–1216 | Symmetric band of $SO_2$ |
| 1453 | Stretching of the C–N band (amid) |
| 700–800 | N–H bending (primary amide) |

The morphology of Cross-PAA-$SO_3H$@nano-$Fe_3O_4$ was determined by Scanning Electronic Microscopy (SEM). It is observed that the particles are strongly aggregated and glued with very large and continuous aggregates (Fig. 3). In order to investigate the size distribution of nanocatalysts [24, 25], dynamic light scattering (DLS) measurements of the nanoparticles were showed in Fig. 4. The size distribution is centered at a value of 52.4 nm. The dispersion for DLS analysis (2.5 g

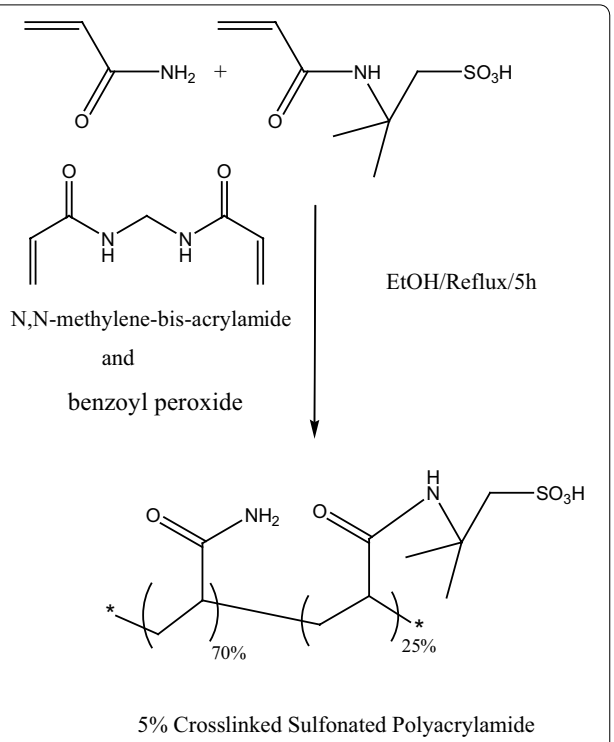


**Scheme 3** Preparation of crosslinked Sulfonated Polyacrylamide (Cross-PAA-$SO_3H$)

nanocatalyst at 50 mL ethanol) was prepared using an ultrasonic bath (60 W) for 30 min.

XRD patterns of Cross-PAA-$SO_3H$, $Fe_3O_4$ and Cross-PAA-$SO_3H$@nano-$Fe_3O_4$ are shown in Fig. 5. The patterns for Cross-PAA-$SO_3H$ indicate a peak at $2\theta = 28°$ which is the most intense peak height (Fig. 5a). All the strong peaks appeared at $2\theta = 30.08°$, 35.40°, 43.17°, 53.59°, 57.20°, 62.86°, and 74.02° can be easily indexed to nano-$Fe_3O_4$ (Fig. 5b). The pattern agrees well with the reported pattern for $Fe_3O_4$ (JCPDS No. 75-1609). The particle size diameter (D) of the nanoparticles has been calculated by the Debye–Scherrer equation ($D = K\lambda/\beta \cos\theta$), where β FWHM (full-width at half-maximum or half-width) is in radian and θ is the position of the maximum of the diffraction peak. K is the so-called shape factor, which usually takes a value of about 0.9, and λ is the X-ray wavelength (1.5406 Å for CuKα). The crystallite size of Cross-PAA-$SO_3H$@nano-$Fe_3O_4$ was calculated by the Debye–Scherer equation is about 48–52 nm. The weaker diffraction lines of Cross-PAA-$SO_3H$@nano-$Fe_3O_4$ (Fig. 5c) compared with $Fe_3O_4$ nanoparticles indicate that the $Fe_3O_4$ nanoparticles were covered by amorphous polymer.

An EDS (energy dispersive X-ray) spectrum of Cross-PAA-$SO_3H$@nano-$Fe_3O_4$ (Fig. 6) exhibits that the elemental compositions are carbon, oxygen, sulfur, iron and nitrogen.

The magnetic attributes of nano-$Fe_3O_4$ and Cross-PAA-$SO_3H$@nano-$Fe_3O_4$ were given with the help of a vibrating sample magnetometer (VSM) (Fig. 7). The amount of saturation-magnetization for nano-$Fe_3O_4$ and Cross-PAA-$SO_3H$@nano-$Fe_3O_4$ is 47.2 emu/g and 26.8 emu/g.

Thermogravimetric analysis (TGA) evaluates the thermal stability of the Cross-PAA-$SO_3H$ and Cross-PAA-$SO_3H$@nano-$Fe_3O_4$. The curve displays a weight loss about 37.5% for Cross-PAA-$SO_3H$@nano-$Fe_3O_4$ from 240 to 550 °C, resulting from the destruction of organic spacer attaching to the nanoparticles. Hence; the nanocatalyst was stable up to 240 °C, confirming that it could be stably utilized in organic reactions at temperatures between the ranges of 80–160 °C (Fig. 8).

### Catalytic behaviors of Cross-PAA-$SO_3H$@nano-$Fe_3O_4$ for the synthesis of 1,3-thiazoles

Initially, we had optimized conditions for the synthesis of 3-alkyl-4-phenyl-1,3-thiazole-2(3*H*)-thione derivatives by the reaction of phenacyl bromide, carbon disulfide and benzyl amine as a model reaction. The model reactions were performed by CAN, $NaHSO_4$, $InCl_3$, $ZrO_2$, *p*-TSA, nano-$Fe_3O_4$, Cross-PAA-$SO_3H$ and Cross-PAA-$SO_3H$@nano-$Fe_3O_4$. The reactions were tested using diverse solvents including ethanol, acetonitrile, water or dimethylformamide. The best results were gained in EtOH and we found that the reaction gave convincing results in the presence of cross-PAA-$SO_3H$@nano-$Fe_3O_4$ (7 mg) under reflux conditions (Tables 2). However, the activity of catalysts is determined by the acid–base properties, surface area, the distribution of sites and the polarity of the surface sites [26, 27]. We studied the feasibility of the reaction by selecting some representative substrates (Table 3). To investigate the extent this catalytic process, phenacyl bromide or 4-methoxyphenacyl bromide, carbon disulfide and primary amine were elected as substrates. Seeking of the reaction scope demonstrated that various primary amines can be utilized in this method (Table 3).

Scheme 4 displays a proposed mechanism for this reaction in the presence of cross-PAA-$SO_3H$@nano-$Fe_3O_4$ as catalyst. Initially the nucleophilic attack by amines on a carbon disulfide generates intermediate (I), The next step involves nucleophilic attack of intermediate (I) on the methylene carbon of phenacyl bromide, leading to intermediate (II), and then ring closure by intramolecular attack of nitrogen at the carbonyl carbon to afford the 3-alkyl-4-phenyl-1,3- thiazole-2(3*H*)-thione derivatives **4**. In this mechanism the surface atoms of cross-PAA-$SO_3H$@nano-$Fe_3O_4$ activate the C=S and C=O groups for better reaction with nucleophiles.

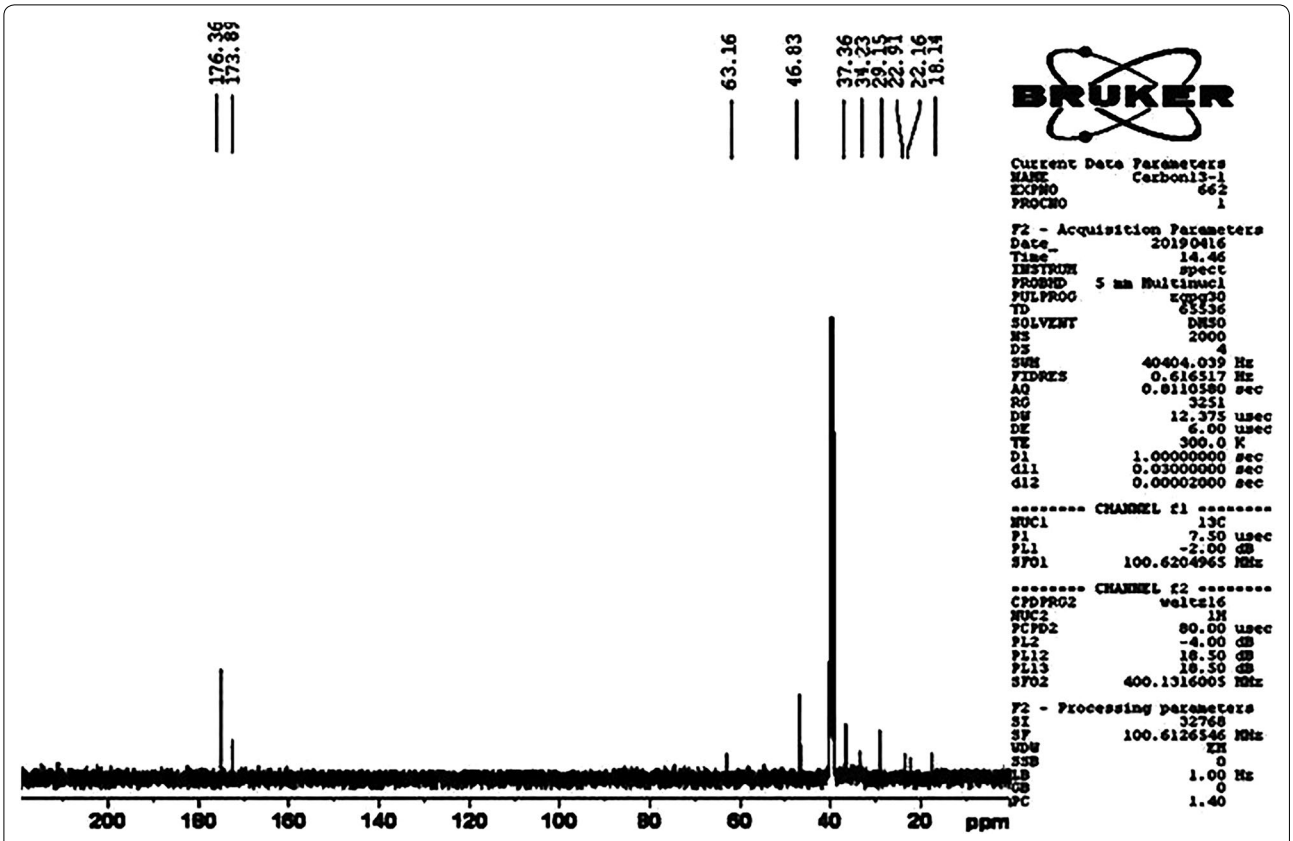


**Fig. 2** The $^{13}C$ NMR spectra of Cross-PAA-$SO_3H$

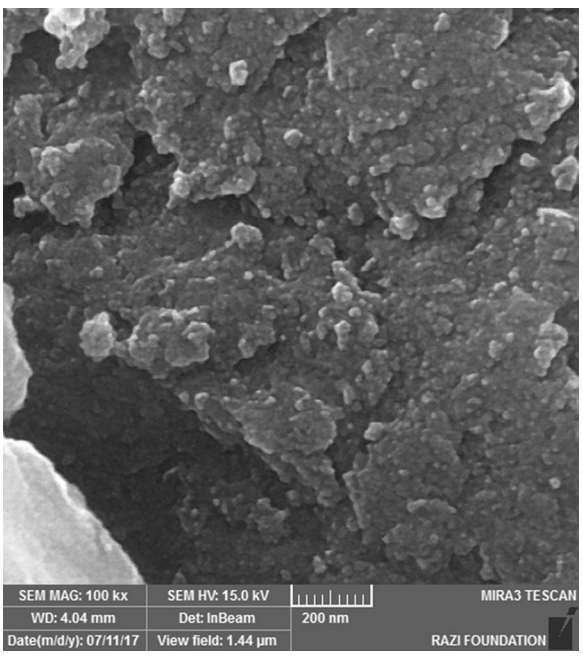


**Fig. 3** SEM image of Cross-PAA-$SO_3H$@nano-$Fe_3O_4$

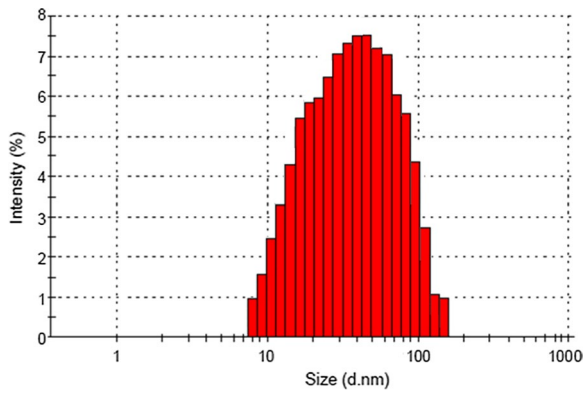


**Fig. 4** The DLS of Cross-PAA-$SO_3H$@nano-$Fe_3O_4$

The reusability of Cross-PAA-$SO_3H$@nano-$Fe_3O_4$ was studied for the reaction of phenacyl bromide, carbon disulfide and benzyl amine and it was found that product yields reduced to a small extent on each reuse (run 1, 94%; run 2, 94%; run 3, 93%; run 4, 93%; run 5, 92%; run 6, 92%;). After completion of the reaction, the

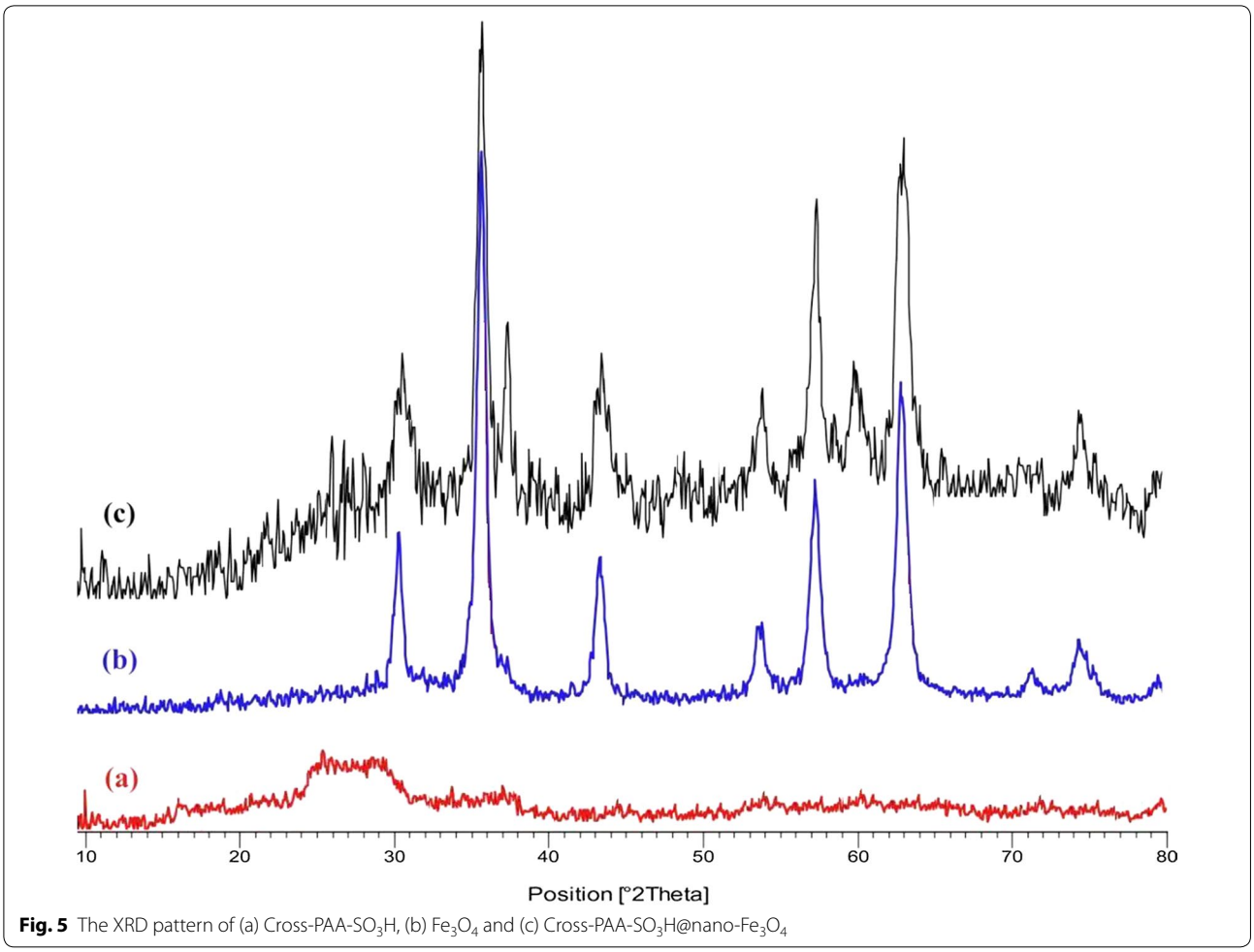


**Fig. 5** The XRD pattern of (a) Cross-PAA-$SO_3H$, (b) $Fe_3O_4$ and (c) Cross-PAA-$SO_3H$@nano-$Fe_3O_4$

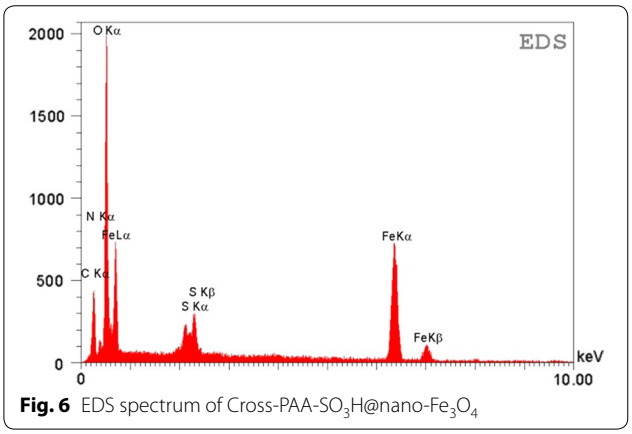


**Fig. 6** EDS spectrum of Cross-PAA-$SO_3H$@nano-$Fe_3O_4$

nanocatalyst was separated by an external magnet. The catalyst was washed four times with ethanol and dried at room temperature for 18 h. The possibility of recycling of the catalyst is an important process from different aspects such as environmental concerns, and commercial applicable processes.

To study the applicability of this method in larger scale synthesis, we performed selected reactions at 10 mmol scale. As can be seen, the reactions at large scale gave the product with a gradual decreasing of reaction yield (Table 4).

To compare the efficiency of Nano $Fe_3O_4$@ PAA-$SO_3H$ with the reported catalysts for the synthesis of 1,3-thiazoles, we have tabulated the results in Table 5. As Table 5 indicates, nano $Fe_3O_4$@ PAA-$SO_3H$ is superior with respect to the reported catalysts in terms of reaction time, yield and conditions. As expected, the increased surface area due to small particle size increased reactivity of catalyst. This factor is responsible for the accessibility of the substrate molecules on the catalyst surface.

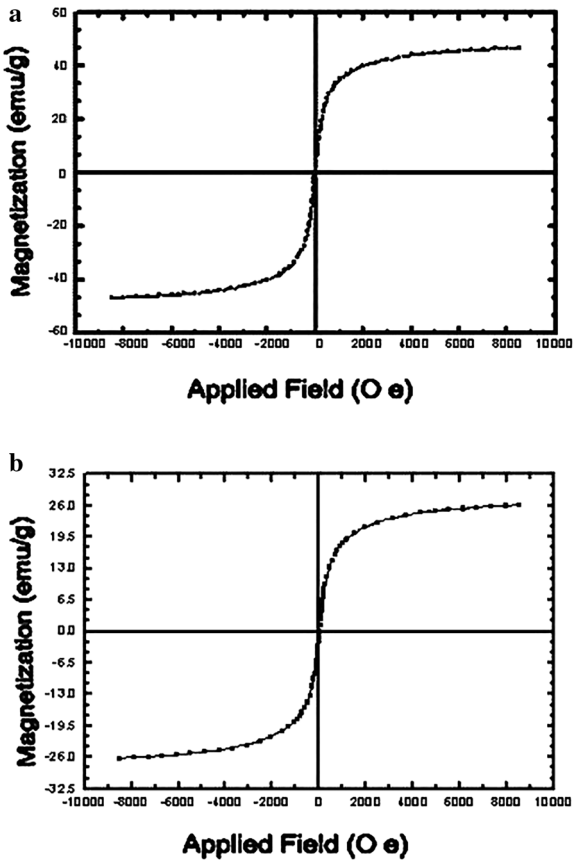


**Fig. 7** The VSM curve of: **a** nano-$Fe_3O_4$ and **b** Cross-PAA-$SO_3H$@nano-$Fe_3O_4$

## Conclusions

In conclusion, we have reported an efficient way for the synthesis of 3-alkyl-4-phenyl-1,3-thiazole-2(3*H*)-thione derivatives using cross-PAA-$SO_3H$@nano-$Fe_3O_4$ under reflux condition in ethanol. The method offers several advantages including easy availability, high yields, shorter reaction times, reusability of the catalyst and low catalyst loading. The present catalytic procedure is extensible to a wide diversity of substrates for the synthesis of a variety-oriented library of thiazoles.

## Experimental section

### Chemicals and apparatus

NMR spectra were obtained on a Bruker spectrometer with $CDCl_3$ as solvent and TMS as an internal standard. Chemical shifts (δ) are given in ppm and coupling constants (J) are given in Hz. FT-IR spectra were recorded with KBr pellets by a Magna-IR, spectrometer 550 Nicolet. CHN compositions were measured by Carlo ERBA Model EA 1108 analyzer. Powder X-ray diffraction (XRD) was carried out on a Philips diffractometer of X'pert Company with monochromatized Cu Kα radiation (λ = 1.5406 Å). Microscopic morphology of products was visualized by SEM (MIRA3). The thermogravimetric analysis (TGA) curves are recorded using a V5.1A DUPONT 2000. The mass spectra were recorded on a Joel D-30 instrument at an ionization potential of

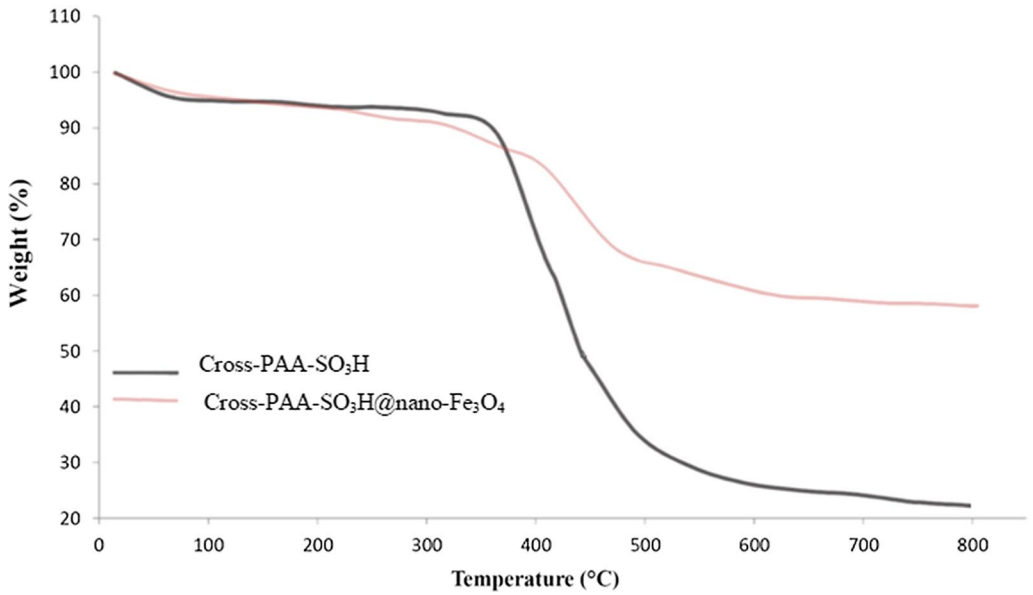


**Fig. 8** TGA curve of Cross-PAA-$SO_3H$ and Cross-PAA-$SO_3H$@nano-$Fe_3O_4$

**Table 2 Optimization of reaction conditions**

| Entry | Solvent (reflux) | Catalyst | Time (min) | Yield (%)[a] |
|---|---|---|---|---|
| 1 | EtOH | – | 500 | 39 |
| 2 | EtOH | CAN (7 mol%) | 250 | 53 |
| 3 | EtOH | $NaHSO_4$ (5 mol%) | 300 | 45 |
| 4 | EtOH | $InCl_3$ (4 mol%) | 200 | 56 |
| 5 | EtOH | $ZrO_2$ (6 mol%) | 250 | 60 |
| 6 | EtOH | *p*-TSA (3 mol%) | 200 | 64 |
| 7 | EtOH | Nano-$Fe_3O_4$ (10 mg) | 200 | 52 |
| 8 | EtOH | Cross-PAA-$SO_3H$ (10 mg) | 150 | 56 |
| 9 | EtOH | nano-$Fe_3O_4$ (5 mg) + Cross-PAA-$SO_3H$ (5 mg) | 150 | 60 |
| 10 | $H_2O$ | Cross-PAA-$SO_3H$@nano-$Fe_3O_4$ (7 mg) | 150 | 77 |
| 11 | DMF | Cross-PAA-$SO_3H$@nano-$Fe_3O_4$ (7 mg) | 150 | 82 |
| 12 | $CH_3CN$ | Cross-PAA-$SO_3H$@nano-$Fe_3O_4$ (7 mg) | 150 | 89 |
| 13 | EtOH | Cross-PAA-$SO_3H$@nano-$Fe_3O_4$ (5 mg) | 150 | 92 |
| 14 | EtOH | Cross-PAA-$SO_3H$@nano-$Fe_3O_4$ (7 mg) | 150 | 94 |
| 15 | EtOH | Cross-PAA-$SO_3H$@nano-$Fe_3O_4$ (9 mg) | 150 | 94 |

Phenacyl bromide (1 mmol), carbon disulfide (1 mmol) and benzyl amine (1 mmol)

[a] Isolated yield

70 eV. The magnetic property of magnetite nanoparticle has been measured with a vibrating sample magnetometer (VSM) (Meghnatis Daghigh Kavir Co.; Kashan Kavir; Iran) at room temperature.

#### *Preparation of crosslinked sulfonated polyacrylamide (Cross-PAA-$SO_3H$)*

In a round-bottom flask (200 mL) equipped with magnetic stirrer and condenser, 5 g of acrylamide (AAM) (70 mmol) and 5.17 g of 2-acrylamido-2-methylpropanesulfonic acid (25 mmol) (AAMPS), [approximately AAM/AAMMPS (3/1)] and 0.77 g of *N*,*N*-methylene-bis-acrylamide (NNMBA) (5 mmol) as crosslinking agent and benzoyl peroxide as initiator were added to 80 mL EtOH under reflux condition for 5 h. After completion of reaction, the white precipitate was formed, filtered, washed and dried in vacuum oven in 70 °C for 12 h. The weight of polymer was 10.1 gr with the yield of 91.8%. Cross-PAA-$SO_3H$ was characterized with infrared spectroscopy and back titration acid–base to confirm sulfonation and determine accurate sulfonation levels. Acidic capacity of this catalyst was estimated 1.1 mmol/g.

#### *Preparation of crosslinked sulfonated polyacrylamide@ nano-$Fe_3O_4$*

1 gr of synthesized polymers were poured in 100 mL round bottom flask under stirring at room-temperature, then 50 mL HCl (0.4 M) was added to it. Our target molecules was synthesized by magnetic nanocatalyst with mass ratio polymer/nano-$Fe_3O_4$ = 2/1. So, 0.43 g (2.1 mol) $FeCl_2{\cdot}4H_2O$ and 1.17 g ($2 \times 2.1$) $FeCl_3{\cdot}6\ H_2O$ were added and the mixture was stirred until dissolved completely (flask1). In another 500 ml round-bottom flask no 2, 400 mL aqueous solution of $NH_3$ (0.7 M) was poured under argon gas. Then flask 1 was added to flask 2 immediately. Nanocatalyst was filtered and washed with water ($2 \times 25$ mL) and dried in oven on 50 °C.

#### *General procedure for the synthesis of 1,3-thiazoles*

A mixture of primary amine (1.0 mmol) and carbon disulfide (1.0 mmol) in ethanol (8 mL) was stirred for 5 min and then phenacyl bromide or 4-methoxyphenacyl bromide (1.0 mmol) and Cross-PAA-$SO_3H$ attached to nano-$Fe_3O_4$ (7 mg) were added, and the mixture was stirred for the appropriate times. The reaction was monitored by TLC (*n*-hexane/ethyl acetate 8:2). After completion of the reaction, the nanocatalyst was easily separated using an external magnet. The solvent was evaporated and the solid obtained washed with EtOH to get pure product. The characterization data of the compounds are given below and in Additional file 1.

*3-Benzyl-4-phenyl-1,3-thiazole-2(3H)-thione* (**4a**) Colorless viscous oil; FT-IR (KBr): $\bar{\nu}$ = 3102, 3005, 1602, 1479, 1202 $cm^{-1}$; $^1H$ NMR (250 MHz, $CDCl_3$): $\delta$ 4.90 (s, 2H, $CH_2$), 6.03 (s, 1H, CH of alkene), 6.95–7.36 (m, 10H, CH, ArH). $^{13}C$ NMR (62.5 MHz, $CDCl_3$): $\delta$

**Table 3 Synthesis of thiazoles using Cross-PAA-$SO_3H$@ nano-$Fe_3O_4$**

| Entry | Amine (R-$NH_2$) | $ArCOCH_2Br$ | Product | Time (min) | Yield (%)[a] |
|---|---|---|---|---|---|
| 1 | 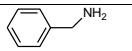 | 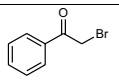 | **4a** | 150 | 94 |
| 2 | 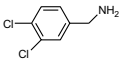 | 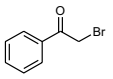 | **4b** | 160 | 87 |
| 3 | 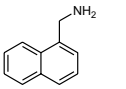 | 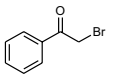 | **4c** | 160 | 86 |
| 4 | 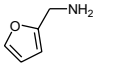 | 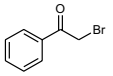 | **4d** | 155 | 92 |
| 5 | 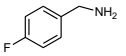 | 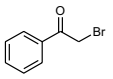 | **4e** | 180 | 90 |
| 6 | 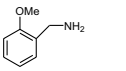 | 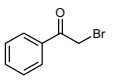 | **4f** | 150 | 94 |
| 7 | 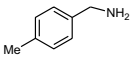 | 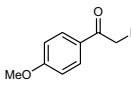 | **4g** | 185 | 89 |
| 8 | 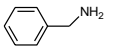 | 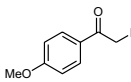 | **4h** | 190 | 84 |
| 9 | 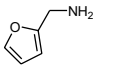 | 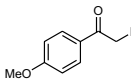 | **4i** | 190 | 82 |
| 10 | 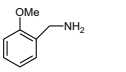 | 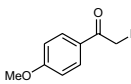 | **4j** | 180 | 88 |

[a] Isolated yield

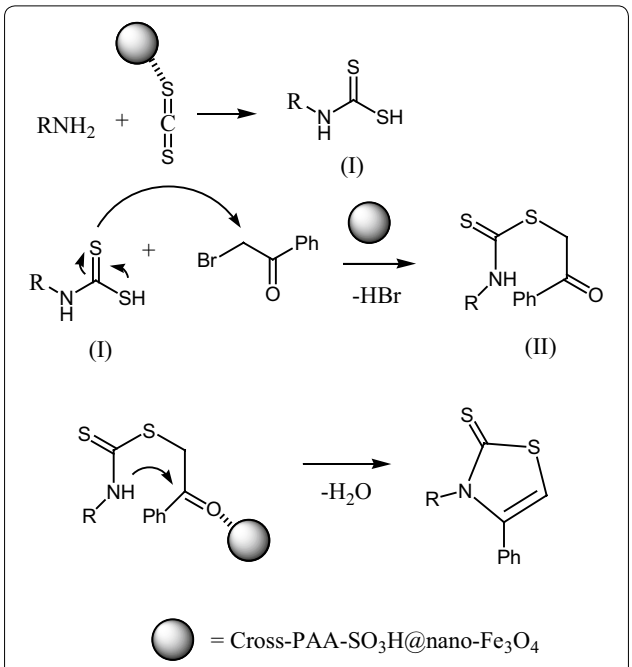


**Scheme 4** Proposed reaction pathway for the synthesis of 1,3-thiazoles

**Table 4 The large-scale synthesis of some 1,3-thiazoles using cross-PAA-$SO_3H$@nano-$Fe_3O_4$**

| Entry | Product | Time (min) | Yield (%)[a] |
|---|---|---|---|
| 1 | **4a** | 200 | 90 |
| 2 | **4e** | 200 | 84 |
| 3 | **4g** | 250 | 82 |
| 4 | **4i** | 250 | 75 |
| 5 | **4j** | 250 | 78 |

47.24, 98.85, 127.06, 127.42, 128.52, 128.55, 129.08, 133.32, 137.45, 154.85, 178.37, 197.18. MS (EI, 70 eV): *m*/*z* (%) = 283 (5), 267 (68), 181 (7), 91 (100), 77 (4), 65 (12), 45 (4). Anal. Calcd. for $C_{16}H_{13}NS_2$ (283): C, 67.81; H, 4.62; N, 4.94. Found: C, 67.70; H, 4.52; N, 4.73%.

*3-(3,4-dichlorobenzyl)-4-phenyl-1,3-thiazole-2(3H)-thione* (**4b**) Colorless viscous oil; FT-IR (KBr): $\bar{\nu}$ = 3152, 3004, 1628, 1603, 1477, 1302, 1104 $cm^{-1}$. $^1H$ NMR (250 MHz, $CDCl_3$): $\delta$ 4.83 (s, 2H, $CH_2$), 6.05 (CH of alkene), 6.75–7.97 (m, 8H, CH of ArH). $^{13}C$ NMR (62.5 MHz, $CDCl_3$): $\delta$ 46.07, 99.25, 126.72, 128.65, 128.74, 129.35, 129.66, 133.54, 130.50, 135.38, 136.62, 137.21, 172.70, 194.15. Anal. Calcd. for $C_{16}H_{11}Cl_2NS_2$ (350): C, 54.55; H, 3.15; N, 3.98. Found: C, 54.36; H, 3.05; N, 3.84%.

*3-(2-Naphthyl methyl)-4-phenyl-1,3-thiazole-2(3H)-thione* (**4c**) Colorless viscous oil; FT-IR (KBr): $\bar{\nu}$ = 3102, 3009, 1652, 1605, 1479, 1204 $cm^{-1}$. $^1H$ NMR (250 MHz, $CDCl_3$): $\delta$ 3.95 (s, 2H, $CH_2$), 6.12 (s, 1H, CH of alkene), 6.92–7.97 (m, 12H, CH of ArH). $^{13}C$ NMR (62.5 MHz, $CDCl_3$): $\delta$ 45.35, 99.05, 123.77, 125.32, 125.84, 126.34, 128.06, 128.68, 128.75, 133.54, 122.52, 129.28, 131.50, 135.08, 172.44, 194.16. Anal. Calcd. for $C_{20}H_{15}NS_2$ (333): C, 72.03; H, 4.53; N, 4.20. Found: C, 72.05; H, 4.40; N, 4.15%.

*3-(2-Furyl methyl)-4-phenyl-1,3-thiazole-2(3H)-thione* (**4d**) Colorless viscous oil; FT-IR (KBr): $\bar{\nu}$ = 3105, 3002, 1653, 1607, 1474, 1202 $cm^{-1}$. $^1H$ NMR (250 MHz,

**Table 5 Comparison of catalytic activity of nano $Fe_3O_4$@ PAA-$SO_3H$ with other reported catalysts for the synthesis 1,3-thiazoles**

| Entry | Catalyst (condition) | Time (min) | Yield[a], % | [Refs] |
|---|---|---|---|---|
| 1 | $Bi(SCH_2COOH)_3$ (15 mol%, 70 °C) | 180 | 80 | [7] |
| 2 | $Yb(OTf)_3$ (15 mol%) | 240 | 60 | [9] |
| 2 | 2-pyridinecarboxaldehyde oxime (20 mol%, DMF) | 400 | 85 | [10] |
| 3 | potassium iodide (10 mol%, $CH_3OH$) | 400 | 80 | [11] |
| 4 | Nano $Fe_3O_4$@ PAA-$SO_3H$ (7 mg, EtOH (under reflux condition) | 150 | 94 | This work |

[a] Isolated yield

$CDCl_3$): $\delta$ 4.84 (s, 2H, $CH_2$), 6.10 (s, 1H, CH of alkene), 6.22 (1H, CH of furan), 7.25–8.05 (m, 7H, CH of ArH and CH of furan). $^{13}C$ NMR (62.5 MHz, $CDCl_3$): $\delta$ 44.25, 98.32, 109.52, 110.83, 127.08, 128.76, 129.58, 142.12, 144.54, 147.92, 155.44, 192.18. Anal. Calcd. for $C_{14}H_{11}NOS_2$ (273): C, 61.51; H, 4.06; N, 5.12. Found: C, 61.46; H, 4.04; N, 5.09%.

*3-(4-Fluorobenzyl)-4-phenyl-1,3-thiazole-2(3H)-thione* (**4e**) Colorless viscous oil; FT-IR (KBr): $\bar{\nu}$ = 3153, 3005, 1628, 1604, 1473, 1302, 1108 $cm^{-1}$. $^1H$ NMR (250 MHz, $CDCl_3$): $\delta$ 4.85 (s, 2H, $CH_2$), 6.05 (s, 1H, CH of alkene), 6.85 (d, 2H, $J$ = 6.8 Hz, CH arom), 7.02–7.59 (m, 5H, CH of ArH), 7.98 (d, 2H, $J$ = 7.5 Hz, CH of ArH).$^{13}C$ NMR (62.5 MHz, $CDCl_3$): $\delta$ 46.45, 99.08, 114.53, 128.67, 128.78, 133.51, 129.05, 135.46, 137.57, 153.28, 159.50, 194.19. Anal. Calcd. for $C_{16}H_{12}FNS_2$ (301): C, 63.76; H, 4.01; N, 4.65. Found: C, 63.60; H, 4.04; N, 4.42%.

*3-(2-Methoxybenzyl)-4-phenyl-1,3-thiazole-2(3H)-thione* (**4f**) Colorless viscous oil; FT-IR (KBr): $\bar{\nu}$ = 3150, 3000, 1650, 1600, 1470, 1200, 1100 $cm^{-1}$. $^1H$ NMR (250 MHz, $CDCl_3$): $\delta$ 3.62 (s, 3H, $OCH_3$), 4.90 (s, 2H, $CH_2$), 6.03 (s, 1H, CH of alkene), 6.71–7.98 (m, 9H, CH, ArH).$^{13}C$ NMR (62.5 MHz, $CDCl_3$): $\delta$ 42.56, 55.05, 98.47, 110.05, 120.53, 128.38, 128.46, 128.55, 128.78, 129.05, 133.54, 127.12, 135.45, 156.35, 194.14. Anal. Calcd. for $C_{17}H_{15}NOS_2$ (313): C, 65.14; H, 4.82; N, 4.47. Found: C, 65.03; H, 4.74; N, 4.35%.

*3-(4-Methylbenzyl)-4-(4-methoxyphenyl)-1,3-thiazole-2(3H)-thione* (**4g**) Colorless viscous oil; FT-IR (KBr): $\bar{\nu}$ = 3156, 3008, 1648, 1612, 1475, 1206, 1108 $cm^{-1}$. $^1H$ NMR (250 MHz, $CDCl_3$): $\delta$ 2.23 (s, 3H, $CH_3$), 3.86 (s, 3H, $OCH_3$), 4.95 (s, 2H, $CH_2$), 5.98 (s, 1H, CH of alkene), 6.82–7.35 (m, 8H, CH of ArH).$^{13}C$ NMR (62.5 MHz, $CDCl_3$): $\delta$ 21.35, 48.54, 55.95, 98.68, 115.38, 123.42, 125.64, 130.65, 131.25, 132.59, 139.25, 160.20, 174.25, 183.56. Anal. Calcd. for $C_{18}H_{17}NOS_2$ (327): C, 66.02; H, 5.23; N, 4.28;. Found: C, 65.90; H, 5.14; N, 4.12%.

*3-benzyl-4-(4-methoxyphenyl)-1,3-thiazole-2(3H)-thione* (**4h**) Colorless viscous oil; FT-IR (KBr): $\bar{\nu}$ = 3157, 3012, 1645, 1616, 1478, 1209, 1107 $cm^{-1}$. $^1H$ NMR (250 MHz, $CDCl_3$): $\delta$ 3.89 (s, 3H, $OCH_3$), 5.25 (s, 2H, $CH_2$), 6.28 (s, 1H, CH of alkene), 6.85–7.39 (m, 9H, CH of ArH).$^{13}C$ NMR (62.5 MHz, $CDCl_3$): $\delta$ 48.50, 55.37, 99.86, 110.55, 114.54, 122.54, 128.38, 129.54, 132.86, 137.54, 145.68, 160.85, 185.36. MS (EI, 70 eV): $m/z$ (%) = 313 (M). Anal. Calcd. for $C_{17}H_{15}NOS_2$ (313): C, 65.14; H, 4.82; N, 4.47; Found: C, 65.02; H, 4.56; N, 4.34; %.

*3-(2-Furyl methyl)-4-(4-methoxyphenyl)-1,3-thiazole-2(3H)-thione* (**4i**) Colorless viscous oil; FT-IR (KBr): $\bar{\nu}$ = 3144, 3012, 1658, 1615, 1478, 1209, 1112 $cm^{-1}$. $^1H$ NMR (250 MHz, $CDCl_3$): $\delta$ 3.88 (s, 3H, $OCH_3$), 4.82 (s, 2H, $CH_2$), 5.98 (2H, CH of furan), 6.20 (s, 1H, CH of alkene), 6.75–7.42 (m, 5H, CH of furan and CH of ArH). $^{13}C$ NMR (62.5 MHz, $CDCl_3$): $\delta$ 41.35, 55.34, 98.36, 108.35, 110.35, 118.35, 122.54, 130.22, 138.54, 142.35, 150.65, 161.25, 178.25. Anal. Calcd. for $C_{15}H_{13}NO_2S_2$ (303): C, 59.38; H, 4.32; N, 4.62; Found: C, 59.15; H, 4.14; N, 4.42. %.

*3-(2-methoxybenzyl)-4-(4-methoxyphenyl)-1,3-thiazole-2(3H)-thione* (**4j**) Colorless viscous oil; FT-IR (KBr): $\bar{\nu}$ = 3142, 3010, 1654, 1611, 1472, 1205, 1116 $cm^{-1}$. $^1H$ NMR (250 MHz, $CDCl_3$): $\delta$ 3.68 (s, 3H, $OCH_3$), 3.84 (s, 3H, $OCH_3$), 4.89 (s, 2H, $CH_2$), 6.05 (s, 1H, CH of alkene), 6.72–7.53 (m, 8H, CH of ArH). $^{13}C$ NMR (62.5 MHz, $CDCl_3$): $\delta$ 43.54, 56.45, 56.48, 98.45, 110.25, 115.28, 120.54, 122.54, 125.85, 125.64, 128.54, 130.42, 138.20, 158.64, 160.24, 172.54. Anal. Calcd. for $C_{18}H_{17}NO_2S_2$ (343): C, 62.94; H, 4.99; N, 4.08; Found: C, 62.72; H, 4.70; N, 3.91. %.

## Supplementary information

**Supplementary information** accompanies this paper at https://doi.org/10.1186/s13065-019-0637-0.

**Additional file 1.** The spectral data of products are described in the additional file 1.

**Abbreviations**
Cross-PAA-$SO_3H$: crosslinked sulfonated polyacrylamide; FT-IR: Fourier-transform infrared spectroscopy; SEM: scanning electron microscope; XRD: X-ray powder diffraction; EDS: energy-dispersive X-ray spectroscopy; TGA: thermogravimetric analysis; VSM: vibrating-sample magnetometer; AAM: acrylamide; AAMPS: 2-acrylamido-2-methylpropanesulfonic acid; DLS: dynamic light scattering.

**Acknowledgements**
The authors acknowledge a reviewer who provided helpful insights.

**Associated content**
Copies of $^1$H-NMR and $^{13}$C-NMR spectra of all compounds are provided in Additional file 1.

**Authors' contributions**
HSHA has designed the study, participated in discussing results and revised the manuscript. MT, JSG and GHM have designed, carried out the literature study, performed the assay, conducted the optimization, purification of compounds and prepared the manuscript. All authors read and approved the final manuscript.

**Funding**
Not applicable.

**Availability of data and materials**
All data generated or analysed during this study are included in this published article [and its additional information files].

**Competing interests**
The authors declare that they have no competing interests.

**Author details**
[1] Young Researchers and Elite Club, Islamic Azad University, Kashan Branch, Kashan, Iran. [2] Department of Organic Chemistry, Faculty of Chemistry, University of Kashan, Kashan, Iran.

Received: 7 June 2019 Accepted: 28 September 2019
Published online: 12 October 2019

**References**

1. Dawood KM, Gomha SM (2015) Synthesis and anti-cancer activity of 1, 3, 4-thiadiazole and 1, 3-thiazole derivatives having 1, 3, 4-oxadiazole moiety. J Heterocyclic Chem 52:1400–1405
2. Abdel-Wahab BF, Abdel-Aziz HA, Ahmed EM (2009) Synthesis and antimicrobial evaluation of some 1,3-thiazole, 1,3,4-thiadiazole, 1,2,4-triazole, and 1,2,4-triazolo[3,4-*b*][1,3,4]-thiadiazine derivatives including a 5-(benzofuran-2-yl)-1-phenylpyrazole moiety. Monatsh Chem 140:601–605
3. Sharma RN, Xavier FP, Vasu KK, Chaturvedi SC, Pancholi SS (2009) Synthesis of 4-benzyl-1, 3-thiazole derivatives as potential anti-inflammatory agents: an analogue-based drug design approach. J Enzyme Inhib Med Chem 24:890–897
4. Maillard LT, Bertout S, Quinonéro O, Akalin G, Turan-Zitouni G, Fulcrand P, Demirci F, Martinez J, Masurier N (2013) Synthesis and anti-Candida activity of novel 2-hydrazino-1, 3-thiazole derivatives. Bioorg Med Chem Lett 23:1803–1807
5. Masquelin T, Obrecht D (2001) A new general three component solution-phase synthesis of 2-amino-1, 3-thiazole and 2, 4-diamino-1, 3-thiazole combinatorial libraries. Tetrahedron 57:153–156
6. Kumar D, Sonawane M, Pujala B, Jain VK, Chakraborti AK (2013) Supported protic acid-catalyzed synthesis of 2, 3-disubstituted thiazolidin-4-ones: enhancement of the catalytic potential of protic acid by adsorption on solid supports. Green Chem 15:2872–2884
7. Foroughifar N, Ebrahimi S (2013) One-pot synthesis of 1, 3-thiazolidin-4-one using Bi $(SCH_2COOH)_3$ as catalyst. Chin Chem Lett 24:383–391
8. Subhedar DD, Shaikh MH, Arkile MA, Yeware A, Sarkar D, Shingate BB (2016) Facile synthesis of 1, 3-thiazolidin-4-ones as antitubercular agents. Bioorg Med Chem Lett 26:1704–1708
9. Su W, Liu C, Shan W (2008) Ytterbium (III) triflate catalyzed one-pot synthesis of 1, 3-thiazolidin-2-imines from epichlorohydrin and thioureas. Synlett 5:725–727
10. Khalaj A, Khalaj M (2016) Organo-catalytic synthesis of 1,3-thiazole derivatives. J Chem Res 40:445–448
11. Safaei-Ghomi J, Salimi F, Ramazani A (2013) The reaction of carbon disulphide with *α*-haloketones and primary amines in the presence of potassium iodide as catalyst. J Chem Sci 125(1087):1092
12. Nayak S, Gaonkar SL (2019) A review on recent synthetic strategies and pharmacological importance of 1,3-thiazole derivatives. Mini-Rev Med Chem 19:215–238
13. Shach-Caplan M, Narkis M, Silverstein MS (2002) Modification of porous suspension-PVC particles by stabilizer-free aqueous dispersion polymerization of absorbed acrylate monomers. Polym Adv Technol 13:151–161
14. Tamami B, Ghasemi S (2010) Palladium nanoparticles supported on modified crosslinked polyacrylamide containing phosphinite ligand: a novel and efficient heterogeneous catalyst for carbon–carbon cross-coupling reactions. J Mol Catal A: Chem 322:98–105
15. Tamami B, Ghasemi S (2011) Modified crosslinked polyacrylamide anchored Schiff base–cobalt complex: a novel nano-sized heterogeneous catalyst for selective oxidation of olefins and alkyl halides with hydrogen peroxide in aqueous media. Appl Catal A Gen 393:242–250
16. Rashidi M, Blokhus AM, Skauge A (2011) Viscosity and retention of sulfonated polyacrylamide polymers at high temperature. J Appl Polym 119:3623–3629
17. Aalaie J, Vasheghani-Farahani E, Rahmatpour A, Semsarzadeh MA (2008) Effect of montmorillonite on gelation and swelling behavior of sulfonated polyacrylamide nanocomposite hydrogels in electrolyte solutions. Eur Polym J 44:2024–2031
18. Kim K, Ju H, Kim J (2016) Surface modification of BN/$Fe_3O_4$ hybrid particle to enhance interfacial affinity for high thermal conductive material. Polymer 91:74–80
19. Low LE, Tey BT, Ong BH, Tang SY (2018) Unravelling pH-responsive behaviour of $Fe_3O_4$@ CNCs-stabilized Pickering emulsions under the influence of magnetic field. Polymer 141:93–101
20. Hyeon T, Lee SS, Park J, Chung Y, Na HB (2001) Synthesis of highly crystalline and monodisperse maghemite nanocrystallites without a size-selection process. J Am Chem Soc 123:12798–12801
21. Harris LA, Goff JD, Carmichael AR, Riffle JS, Harburn JJ, Pierre TG, Saunders M (2003) Magnetite nanoparticle dispersions stabilized with triblock copolymers. Chem Mater 15:1367–1377
22. Lutz JF, Stiller S, Hoth A, Kaufner L, Pison U, Cartier R (2006) One-pot synthesis of pegylated ultrasmall iron-oxide nanoparticles and their in vivo evaluation as magnetic resonance imaging contrast agents. Biomacromol 7:3132–3138
23. Mincheva R, Stoilova O, Penchev H, Ruskov T, Spirov I, Manolova N, Rashkov I (2008) Synthesis of polymer-stabilized magnetic nanoparticles and fabrication of nanocomposite fibers thereof using electrospinning. Eur Polym J 44:615–627
24. Bootz A, Vogel V, Schubert D, Kreuter J (2004) Comparison of scanning electron microscopy, dynamic light scattering and analytical ultracentrifugation for the sizing of poly(butylcyanoacrylate) nanoparticles. Eur J Pharm Biopharm 57:369–375
25. Na K, Zhang Q, Somorjai GA (2014) Colloidal metal nanocatalysts: synthesis, characterization, and catalytic applications. J Clust Sci 25:83–114
26. Safaei-Ghomi J, Shahbazi-Alavi H, Heidari-Baghbahadorani E (2014) SnO nanoparticles as an efficient catalyst for the one-pot synthesis of chromeno[2,3-b]pyridines and 2-amino-3,5-dicyano-6-sulfanyl pyridines. RSC Adv. 4:50668–50677
27. Safaei-Ghomi J, Shahbazi-Alavi H (2017) Synthesis of dihydrofurans using nano-$CuFe_2O_4$@ Chitosan. J Saudi Chem Soc 21:698–707

## Publisher's Note